

Broadband Circularly Polarized Antenna by Using Polarization Conversion Metasurface

Zi-Jian Han^{1,2}, Wei Song^{1*}, and Xin-Qing Sheng¹

¹Center for Electromagnetic Simulation, School of Information Science and Technology
Beijing Institute of Technology, Beijing 100081, China
wsong@bit.edu.cn

²Beijing Institute of Space Long March Vehicle, Beijing 100076, China

Abstract — A compact and broadband circularly polarized antenna is proposed. A linear-to-circular polarization conversion metasurface is designed to broaden the 3-dB axial ratio bandwidth and the impedance bandwidth of the proposed antenna, with the mechanism of the metasurface investigated. Different with the conventional metasurface antenna designed by using uniform unit cells, this design makes use of two metasurface arrays with different unit cells. Full wave simulations show that the 10-dB impedance bandwidth of the proposed antenna is from 4.32 to 6.5 GHz (40.3%), and the 3-dB AR bandwidth is from 5 to 5.61 GHz (11.5%). Compared with that using the uniform elemental array, this design leads to more than 10% improvement in the 10-dB impedance bandwidth and more than 11.7% improvement in the axial ratio bandwidth. The proposed antenna has been fabricated and the simulated results have been verified with the measurements.

Index Terms — Circularly polarized antenna, linear-to-circular polarization conversion, metasurface.

I. INTRODUCTION

Metasurface (MS) has attracted much attention due to its unique properties in the past few years [1]. It is usually formed by regular or irregular periodic planner arrays and presents EM properties not found in natural materials. With advantages of planar structure and strong capability of manipulating electromagnetic waves, MS can be easily integrated on traditional antennas and provide a promising approach for new antenna designs with improved performances [2-13].

For radar, wireless, and satellite communication applications, circularly polarized (CP) antennas [14, 15] are widely used because of their immunities to multipath distortion and polarization mismatch losses. MS can be utilized to improve the CP performance or to convert a linearly polarized radiation from antennas to a circularly polarized one without deteriorating the radiation

performance [3]. Dual-band conversion can also be realized by a single metasurface [4]. By properly combining the transmitted wave from the antenna and the reflected wave from the metasurface, broadband circular polarization can be obtained [5-7]. In [8-10], the metasurfaces work as polarization converters and the E-field can be resolved into two orthogonal components. In this way, the circularly polarized wave can be possibly generated with wider bandwidth. In order to enhance the impedance-matching and the AR bandwidths, surface waves are excited on the MS to generate additional resonances with minimum AR points [11, 12]. Based on the mushroom antenna [1], a new wideband CP antenna can be realized by rotating the angle of the feed slot for a polarization-dependent MS superstrate [13].

The above MS antennas are all based on periodic MS arrays with the same unit cells. In this paper, we demonstrate by combining two linear-to-circular polarization conversion MS (PCMS) arrays, the 3-dB axial ratio (AR) bandwidth and impedance bandwidth can be further broadened. Simulation shows that the 10-dB impedance bandwidth for the proposed MS antenna is 40.3% from 4.32 to 6.5 GHz, and the 3-dB AR bandwidth is 11.5% from 5 to 5.61 GHz. Compared with the same element array, more than 10% improvement for 10-dB impedance bandwidth and more than 11.7% improvement for 3-dB AR bandwidth can be obtained. As the design verification, the proposed antenna is fabricated and measured. The measurement results agree with the simulation results.

II. ANTENNA DESIGN

A. Linear-to-circular polarization conversion MS

A linear-to-circular PCMS is made of arrays of the unit cell as shown in Fig. 1 (a). The unit cell consists of a metallic patch with a 45 degree-oriented rectangular slot and a substrate board with the thickness of 3 mm and the relative permittivity of 4.4. The dimensions of the unit cell specified in Fig. 1 (a) are as follows:

$px = py = 11\text{mm}$, $l = w = 10\text{mm}$, $ls = 11\text{mm}$, and $ws = 0.65\text{mm}$. Consider an x-polarized plane wave normally illuminated on the bottom of the PCMS. This means the incidence only contains Ex component. The amplitudes of the transmitted E-field components are simulated by commercial software Ansoft HFSS. Master/slave boundaries are utilized based on a unit-cell model. The simulation results show that the amplitude intersections of Ex and Ey can be obtained and the corresponding frequency of the matching point varies with the length of the slots on the patch (Ref. Fig. 1 (b)).

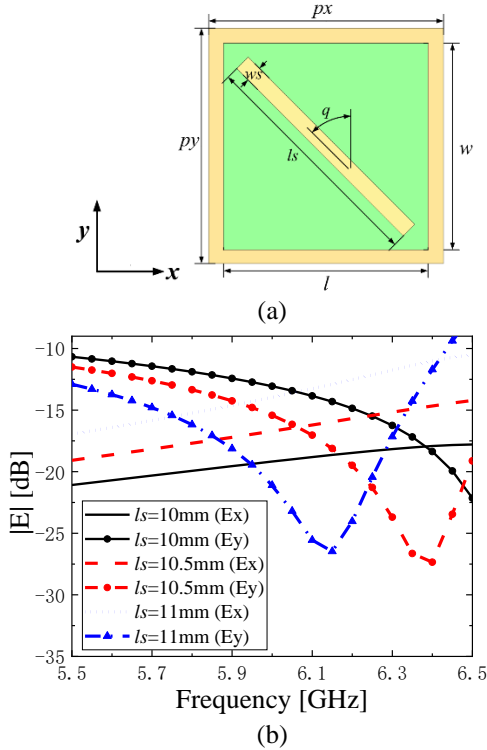


Fig. 1. (a) A unit cell of the PCMS, and (b) the amplitudes of the transmitted E-field components.

This indicates that, after the x-polarized plane wave transmits through the MS, both Ex and Ey components are generated with equal amplitudes in the transmitted wave. In this way, circularly polarized wave can be possibly generated when the MS array is properly designed. Accordingly, by considering the PCMS as a half-wavelength resonant cavity, the resonant length of slot can be qualitatively estimated by the following equation

$$ls = \lambda_e / 2 = \lambda / 2\sqrt{\epsilon_r}, \quad (1)$$

where ls is the wavelength in the dielectric substrate and ϵ_r is the relative permittivity of the substrate.

As shown in Fig. 2, at 5.75GHz, the currents on slot with $ls = 11\text{mm}$ are better excited than that on slot with $ls = 10\text{mm}$, which further verifies the linear-to-circular

polarization conversion function of the slot.

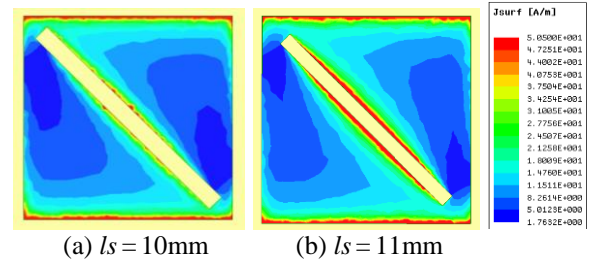


Fig. 2. Simulated surface current amplitudes of the PCMS at 5.75 GHz for different slot lengths.

B. CP Antenna incorporating two CPMSs

Based on a MS-based broadband low-profile mushroom antenna as presented in [1], by simply replacing the mushroom EBG with the aforementioned PCMS arrays on a planar slot-coupling antenna, we obtain the proposed CP antenna. In order to obtain broader 3-dB AR and impedance bandwidths, the 4 by 4 PCMS array are separated into two 2 by 4 arrays as depicted in Fig. 3. After optimization, the dimension parameters of the PCMS arrays are determined as follows (in unit of mm): $l = 8.25$, $w = 8$, $px = 9.45$, $py = 9.2$, $ls1 = 9.45$, $ws1 = 0.65$, $ls2 = 8.8$, and $ws2 = 0.65$. The tilt angles for the two CPMSs are $q1 = 52.5^\circ$ and $q2 = 57^\circ$ respectively. The parameters of the feeding slot antenna are (in unit of mm): $le = 25$, $we = 2$, $lf = 27.5$, $wf = 2.1$, $lg = 16$, $wg = 5$, and $gf = 1.55$. Here, FR4 ($\epsilon_r = 2.2$) is used as substrate for both the PCMS and the antenna. The thicknesses of the PCMS substrate and the antenna substrate are $h = 3\text{mm}$ and $t = 1\text{mm}$ respectively. A waveguide port is assigned to the coplanar waveguide as excitation in the HFSS model as shown in Fig. 3 (b). Figure 4 (a) shows the simulated S11 for the MS antenna. The simulated impedance bandwidth for $S11 < -10\text{ dB}$ is 4.32–6.5 GHz (40.3%). Figure 4 (b) shows the simulated axial ratio and gain in the boresight direction for the proposed antenna. It shows the PCMS array resulted in stable left-hand circular polarization (LHCP) radiation. The 3-dB AR bandwidth is from 5 to 5.61 GHz, about 11.5%. In Fig. 4 (c) the simulated radiation patterns of the proposed antenna at 5.3 GHz is provided.

The simulation results show that, as the time changes, the surface currents located at the azimuth angle turn in a clockwise manner. Figure 5 shows snapshots of the surface currents of the proposed antenna at 5.2 GHz for three different time phases (ωt), from 0° to 90° , with an interval of 45° . At $\omega t = 0^\circ$, the dominant surface current can be found in the y-direction, while as ωt changes to $\omega t = 45^\circ$ and then $\omega t = 90^\circ$, the dominant surface currents can be observed in the diagonal direction and then in the x-direction. Hence, the polarization characteristic is the LHCP in +z-direction.

It also can be seen in Fig. 5 that the current intensities on PCMS on different locations are different. It is understood that the discrepancy in the unit cells of CPMSs will decrease the resonance of the CPMSs in the center zone where strong mutual coupling occurs, however, strong resonance can still be formed on the edge of the structure, rendering the improved antenna performance.

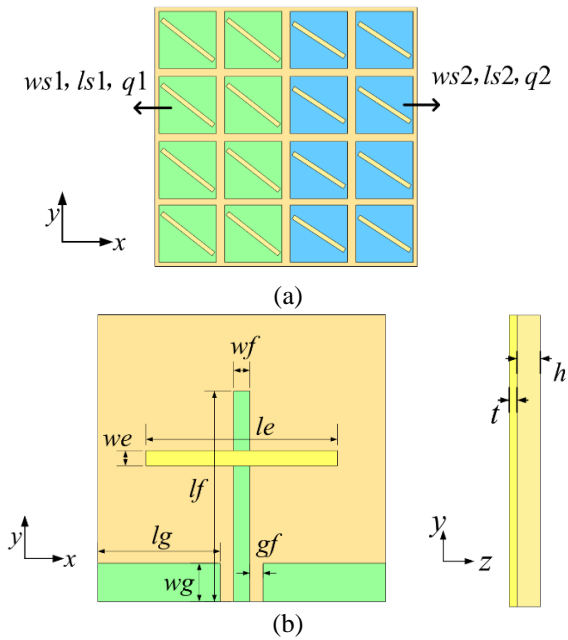


Fig. 3. Illustration of the geometry with the design parameters of the proposed antenna: (a) the top view; (b) the back view and the side view.

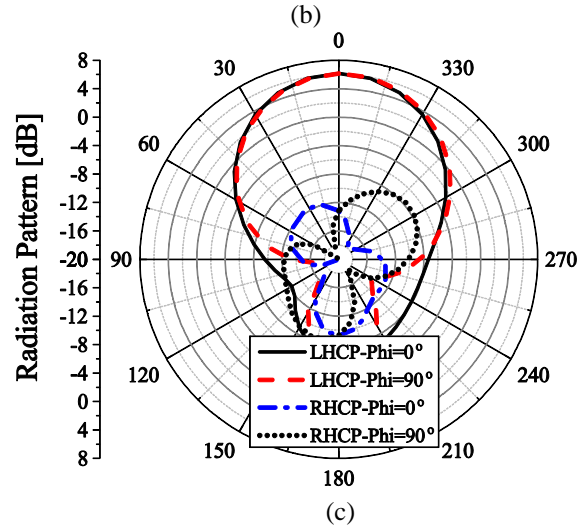
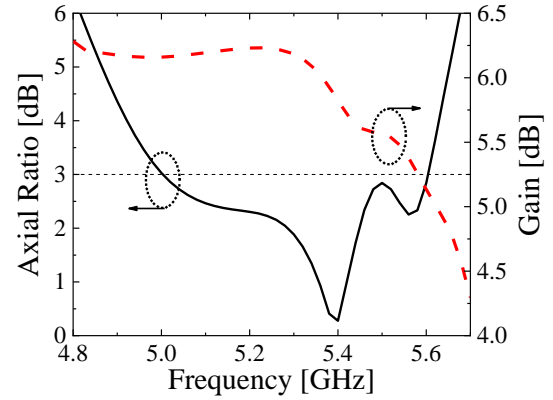
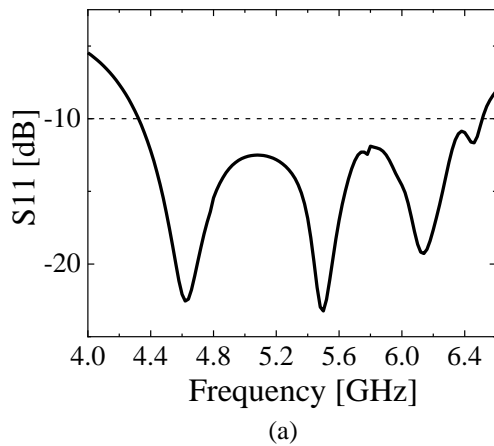
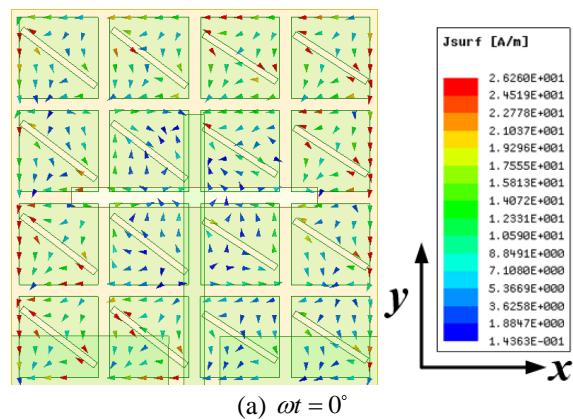


Fig. 4. (a) The simulated S_{11} , (b) AR and broadside gain, and (c) the radiation pattern at 5.3GHz of the proposed antenna.



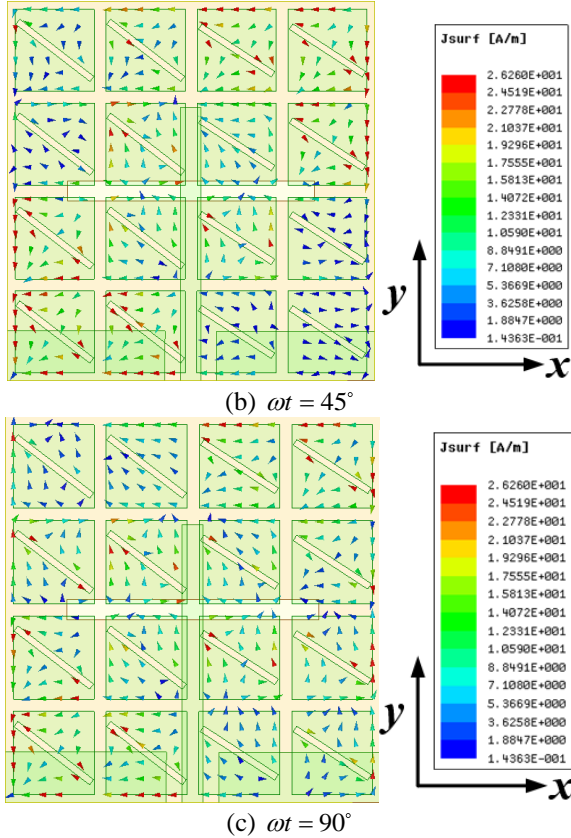


Fig. 5. Simulated surface current distributions of the proposed antenna at 5.3 GHz for different time instants.

III. EXPERIMENTAL RESULTS

In Fig. 6, the simulated axial ratio (AR), the broadside gain, and the S11 parameter of the proposed antenna based on two different dimensions of PCMS arrays are compared with those of the two antennas with uniform PCMS arrays. The key parameters which are different among the three antennas are specified in the figure. The rest parameters are the same with those in Section II. It can be seen that wider 3-dB AR bandwidth and impedance bandwidth can be achieved by properly adjusting the length and rotating the angle (in degrees) of the rectangular slots without deteriorating the radiation performance. Parametric studies are performed to identify the effect of separating to two PCMS arrays on the impedance bandwidth, AR bandwidth in the boresight direction and the results provide a useful strategy to broaden the bandwidth for practical design. Compared with the antenna used for same elements with the wider bandwidth, more than 10% improvement for 10-dB impedance bandwidth and more than 11.7% improvement for 3-dB AR bandwidth can be obtained by adopting the combination of the two PCMS arrays.

The proposed antenna as shown in Fig. 7 is etched on FR4 substrate with a relative permittivity of 4.4 and a loss tangent of 0.02. Its characteristics are measured as design verification. As depicted in Figs. 8 (a) and (b), the measured results show that the 10-dB impedance bandwidth for the proposed MS antenna is 38.3% from 4.56 to 6.72 GHz, and the 3-dB AR bandwidth is 11.3% from 5 to 5.6 GHz. Figures 8 (c) and (d) show the simulated and measured radiation patterns at 5.3GHz. As can be found in Fig. 8, the measured results show good agreement with the simulated ones, and the deviations could be attributed to the fabrication and measurement tolerance.

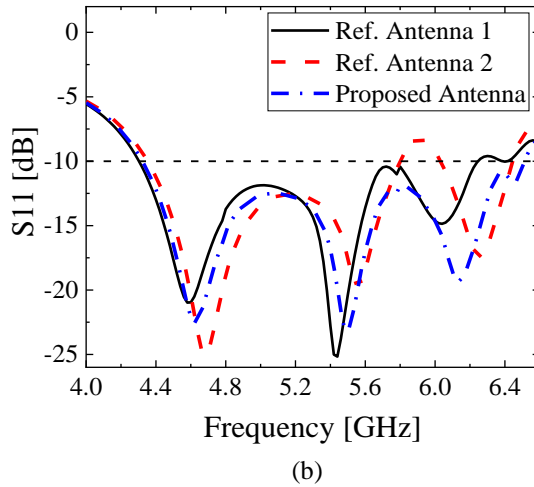
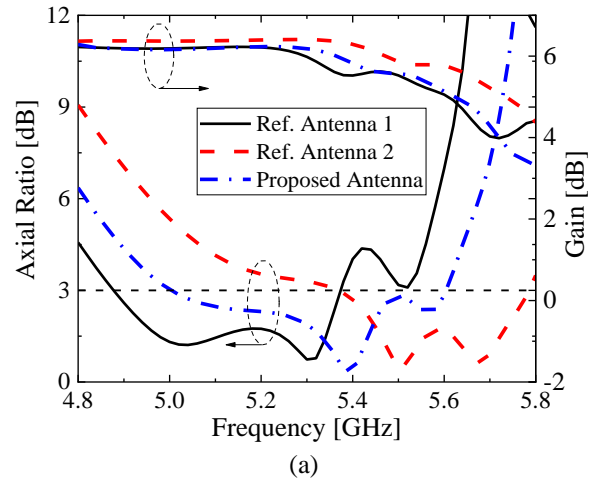


Fig. 6. (a) The AR, broadside gain and (b) the S11 of the proposed antenna and the two reference antennas with uniform PCMS array (the proposed antenna: $(l_1, l_2, q_1, q_2) = (9.45\text{mm}, 8.80\text{mm}, 52.5^\circ, 57^\circ)$; Ref. Antenna 1: $(l_1, q_1) = (9.45\text{mm}, 52.5^\circ)$; Ref. Antenna 2: $(l_2, q_2) = (8.80\text{mm}, 57^\circ)$).

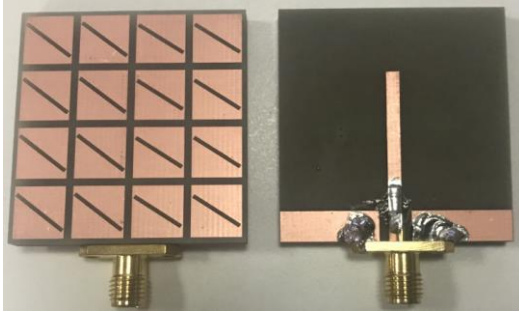
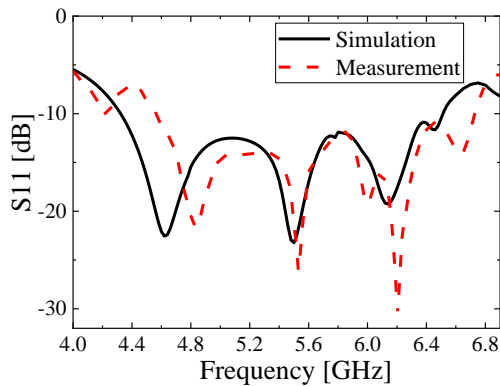
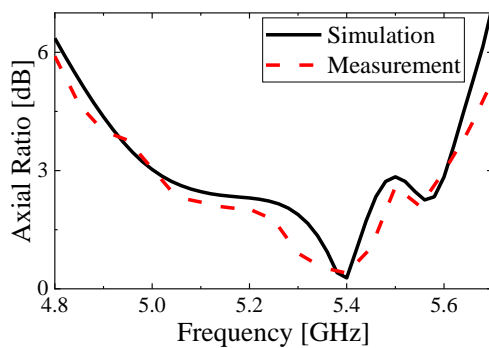


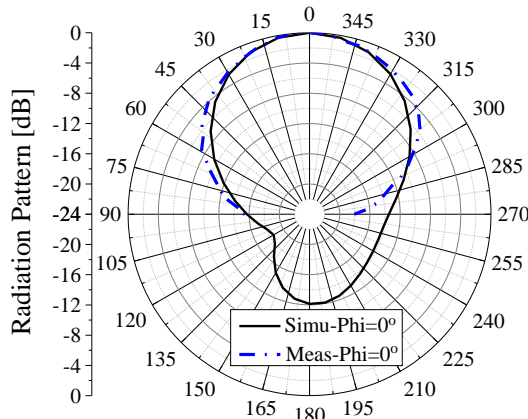
Fig. 7. Photographs of the fabricated antenna prototype.



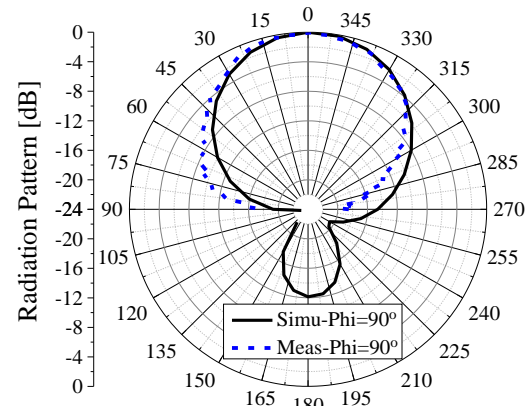
(a)



(b)



(c)



(d)

Fig. 8. (a) The S11, (b) the axial ratio, (c) the radiation patterns normalized by maxima at 5.3 GHz of the proposed antenna at $\varphi=0^\circ$ plan, and (d) the radiation patterns normalized by maxima at 5.3 GHz of the proposed antenna at $\varphi=90^\circ$ plan.

IV. CONCLUSION

An efficient method is presented to broaden the 3-dB AR bandwidth and the impedance bandwidth based on two PCMS arrays with different parameters in this paper. The proposed antenna design exhibits more than 10% improvement for 10-dB impedance bandwidth and more than 11.7% improvement for the 3-dB AR bandwidth compared with that composing the PCMS array with uniform elements. The simulated and measured results are in good agreement to verify the proposed antenna.

ACKNOWLEDGMENT

This work is supported by the National Key R&D Program of China under Grant 2017YFB0202500, and the NSFC under Grant No. 61601023 and U1730102.

REFERENCES

- [1] W. Liu, Z.-N. Chen, and X. Qing, "Metamaterial-based low-profile broadband mushroom antenna," *IEEE Trans. Antennas Propag.*, vol. 62, no. 3, pp. 1165-1172, 2013.
- [2] Z.-J. Han, W. Song, and X.-Q. Sheng, "Gain enhancement and RCS reduction for patch antenna by using polarization-dependent EBG surface," *IEEE Antennas Wireless Propag. Lett.*, vol. 16, pp. 1631-1634, 2017.
- [3] F. Yang and Y. Rahmat-Samii, "A low profile single dipole antenna radiating circularly polarized waves," *IEEE Trans. Antennas Propag.*, vol. 53, no. 9, pp. 3083-3086, 2005.
- [4] H. Yi and S.-W. Qu, "A novel dual-band circularly polarized antenna based on electromagnetic band-

- gap structure," *IEEE Antennas Wireless Propag. Lett.*, vol. 12, pp. 1149-1152, 2013.
- [5] H.-P. Li, G.-M. Wang, J.-G. Wang, and X.-J. Gao, "Wideband multifunctional metasurface for polarization conversion and gain enhancement," *Progress In Electromagnetic Research*, vol. 155, pp. 115-125, 2016.
- [6] T. Nakamura and T. Fukusako, "Broadband design of circularly polarized microstrip patch antenna using artificial ground structure with rectangular unit cells," *IEEE Trans. Antennas Propag.*, vol. 59, no. 6, pp. 2103-2110, 2011.
- [7] S. Maruyama and T. Fukusako, "An interpretative study on circularly polarized patch antenna using artificial ground structure," *IEEE Trans. Antennas Propag.*, vol. 62, no. 11, pp. 5919-5924, 2014.
- [8] H.-L. Zhu, S.-W. Cheung, K.-L. Chung, et al., "Linear-to-circular polarization conversion using metasurface," *IEEE Trans. Antennas Propag.*, vol. 61, no. 9, pp. 4615-4623, 2013.
- [9] H.-L. Zhu, S.-W. Cheung, K.-L. Chung, et al., "Design of polarization reconfigurable antenna using metasurface," *IEEE Trans. Antennas Propag.*, vol. 62, no. 6, pp. 2891-2898, 2014.
- [10] C. Chen, Z. Li, L.-L. Liu, J. Xu, P. Ning, B. Xu, X. Chen, and C.-Q. Gu, "A circularly-polarized metasurfaced dipole antenna with wide axial-ratio beamwidth and RCS reduction functions," *Progress In Electromagnetics Research*, vol. 154, pp. 79-85, 2015.
- [11] S.-X. Ta and I. Park, "Low-profile broadband circularly polarized patch antenna using metasurface," *IEEE Trans. Antennas Propag.*, vol. 63, no. 12, pp. 5929-5934, 2015.
- [12] S.-X. Ta and I. Park, "Compact wideband circularly polarized patch antenna array using metasurface," *IEEE Antennas Wireless Propag. Lett.*, vol. 16, pp. 1932-1936, 2017.
- [13] Z. Wu, L. Li, Y. Li, et al., "Metasurface superstrate antenna with wideband circular polarization for satellite communication application," *IEEE Antennas Wireless Propag. Lett.*, vol. 15, pp. 374-377, 2016.
- [14] M. I. Sabran, S. K. A. Rahim, P. J. Soh, C. Y. Leow, and G. Vandenbosch, "A simple electromagnetically fed circularly-polarized circular microstrip antenna," *Applied Computational Electromagnetics Society Journal*, vol. 30, no. 11, pp. 1180-1187, 2015.
- [15] M. Shokri, S. Asiaban, and Z. Amiri, "Study, design and fabrication of a cpw fed compact monopole antenna with circular polarization for ultra wide band systems application," *Applied Computational Electromagnetics Society Journal*, vol. 32, no. 9, pp. 749-753, Sep. 2017.